Energy 254 (2022) 123719

Contents lists available at ScienceDirect

Energy

journal homepage: www.elsevier.com/locate/energy

Model-based design validation and optimization of drive systems in electric, hybrid, plug-in hybrid and fuel cell vehicles

Désirée Alcázar-García*, José Luis Romeral Martínez

Universitat Politècnica de Catalunya, Carrer de Jordi Girona, 31, 08034, Barcelona, Spain

ARTICLE INFO

Article history:
Received 5 July 2021
Received in revised form
9 March 2022
Accepted 10 March 2022
Available online 23 March 2022

Keywords:
Design optimization
Electric vehicle
Energy consumption
Fuel cell vehicle
Genetic algorithm
Hybrid electric vehicle
Micromobility
Vehicle configuration
Vehicle efficiency

ABSTRACT

We are currently immersed in the fourth industrial revolution, which involves, among others, technology to prevent climate change, transformation of the transport sector, digitization, and artificial intelligence. This paper contributes to technological development accelerating the design of ecological vehicles and their introduction in smart cities.

This paper describes an adaptive, flexible, expandable, simple, and high-accuracy methodology capable of maximizing vehicle range with the finest computational effort, thanks to a genetic algorithm. Further, it produces predictive information to minimize cost, volume, and weight of the drivetrain in the vehicle structure while meeting the desires of the designer.

Range is calculated using a standard or customised drive cycle. Calculation of the CO_2 produced in the electricity production process is also provided. The reliability of the system has been verified with commercially available vehicles, taking into account their technical specifications such as electric motor type (e.g. induction, permanent magnet, or hybrid electric motors), the technology of the energy storage system (e.g. nickel-metal hydride or lithium-ion batteries or fuel cell), configuration (e.g. pure electric vehicle, series/parallel/series-parallel (plug-in) hybrid electric vehicle, or fuel cell vehicle) and their category (light quadricycles [L6e], heavy quadricycles [L7e], passenger cars [M_1], vans [N_1], or low-speed vehicles). The results obtained demonstrate that the model is capable of extraordinary precision.

1. Introduction

The transport sector is responsible for 25% of all CO_2 emissions worldwide. In particular, the energy required to operate personal vehicles represents a significant contribution of greenhouse gas emissions per capita due to the large ownership and use of internal combustion engine (ICE) vehicles. This share can be greatly reduced by obtaining the energy needed for transportation from renewable sources [1].

This percentage will surely increase, as motorization rates, with ICE vehicles, which contribute substantially to air pollution, are increasing worldwide. In this context, there is increasing interest in zero-carbon-emission power to prevent global warming. Mobility electrification may become a viable option for light road transportation since it removes or minimizes damaging emissions directly from urban areas and relies on electricity as an energy vector, which can help decouple transportation from oil consumption [2,3].

Approximately 14% of the growth in energy use is offset by energy efficiency improvements, and its effect is limited in the public transportation sector, compared with the private passenger vehicle sector [4].

Advanced technologies such as vehicle electrification and the integration of electric vehicle (EV) components have gained a prominent interest and are recognized as an effective way to reduce vehicle fuel consumption and emissions. These designs offer valid, suitable, and sensible solutions that practically eliminate the negative impact of vehicles, especially on urban air quality, and provide an on-demand, high torque, with less noise and smoother acceleration and deceleration as compared to the ICE vehicles [5,6].

One of the solutions to tackle the problem of vehicle emissions is to promote green mobility such as electric, hybrid and fuel cell vehicles (FCVs). According to [7], 45% of the on-road electric vehicles are in China, 24% are in Europe, and the United States accounts for 22%. As mentioned, next-generation vehicles are emerging in response to environmental pressures and a goal of fuel independence. Fuel independence requires removing reliance on fossil fuels

* Corresponding author.
E-mail address: Desiree.Alcazar@upc.edu (D. Alcázar-García).

https://doi.org/10.1016/j.energy.2022.123719
0360-5442/

Nomenclature

Abbreviations	
AC	alternating current
AESC	Automotive Energy Supply Corporation
BEV	battery electric vehicle
BMS	battery management system
BMW	bayerische Motoren Werke
CO_2	carbon dioxide
DC	direct current
DP	dynamic programming
ECE-15	urban driving cycle (or UDC)
EPA	environmental protection agency
ESS	energy storage system
EU	European Union
EV	electric vehicle
FC	fuel cell
FCEV	fuel cell electric vehicle
FCV	fuel cell vehicle
GA	genetic algorithm
HEV	hybrid electric vehicle
HWFET	highway fuel economy test
ICE	internal combustion engine
IM	induction motor
IPM	interior permanent magnet
JC08	Japan cycle'08
LCO	$LiCoO_2$
LFP	$LiFePO_4$
Li-ion	lithium-ion
LMO	$LiMn_2O_4$
LNO	$LiNiO_2$
LSV	low-speed vehicle
LTO	$Li_4Ti_5O1_2$
NCA	$LiNi_xCo_xAl_xO_2$
NEDC	new European driving cycle
NiMH	nickel-metal hydride
NMC	$LiNi_xMn_xCo_xO_2$
OEM	original equipment manufacturer
PEMFC	proton exchange membrane fuel cell
PHEV	plug-in hybrid electric vehicle
PSO	particle swarm optimization
SA	simulated annealing
SCV	specific calorific value
SPM	surfaced permanent magnet
UDC	urban driving cycle (or ECE-15)
UK	United Kingdom
VW	Volkswagen
WLTP	world harmonized light-duty vehicle test procedure
Symbols	
A	frontal area of the car [m^2]
a	acceleration of the car [m/s^2]
α	angle of the slope [°]
c_w	drag coefficient [no units]
ρ	density of the air [kg/m^3]
E	consumed energy
ε	error
€	euro
F_{Si}	climbing resistance [N]
F_L	drag resistance [N]
F_{R0}	rolling resistance [N]
F_T	running resistance [N]
f	rolling resistance coefficient [no units]
ξ_n	gear ratios [no units]
g	gravity [m/s^2]
km	kilometre
l	litre
m	mass of the vehicle [kg]
θ_{wheel}	mass moment of inertia of the wheel [$kg \cdot m^2$]
θ_n	mass moments of inertia of the rotating components [$kg \cdot m^2$]
P	power [W]
η	power losses of vehicle parts [%]
r_{wheel}	rolling radius of the wheel [m]
t	drive cycle time [s]
v	speed of the vehicle [m/s]
v_0	speed of the wind [m/s]

and the geopolitics associated with sourcing petroleum. Direct and indirect electrification technologies such as battery electric vehicles (BEVs) and FCV using renewable hydrogen from water electrolysis are the two emerging options to power alternative vehicles [8,9].

As an example of this commitment, governments are beginning to legislate [10]. For instance, the European Union may ban production and sale of ICE vehicles as shown in Table 1 [11].

One way of contributing to the technological development demanded by the modern world is by developing a method to accelerate and facilitate the design and sizing of no-fossil-fuel and ecological vehicles, focusing on their configuration, powertrain, and energy storage system (ESS).

1.1. Literature review

This paper presents a simplified but precise and accurate procedure to design and size the ESS and electric motor that can be used interchangeably for any 4-wheeled EV, hybrid electric vehicle (HEV), PHEV (plug-in HEV), and FCV that belongs to the category of light quadricycles (L6e), heavy quadricycles (L7e), passenger cars (M_1), vans (N_1) or low-speed vehicles (LSVs). For that purpose, it will be necessary to know the energy consumption, grams of CO_2 emissions, and the technology, costs, weight, and volume of different components, all while considering different system configurations, their individual efficiencies, and customised or standard drive cycles.

A new procedure of sizing and selecting technologies for parts like the ESS and electric motor is presented. No other reference has been found in all the reviewed literature that includes a similar methodology with the same degree of flexibility in the design process considering the whole vehicle, and different configurations and categories.

This topic has been tackled partially from other perspectives by other authors but with different methodologies. These studies lack validation of the results with real vehicles beyond a prototype. The methodology presented herein is more complete, more flexible,

Table 1
Select national government targets for phasing out combustion engine cars up to 2040 and selected implementation policies as of April 2020.

Country	Phase-out year	Policy document	Target according to policy document
Norway	2025	National Transport Plan 2018–2029	All new passenger cars and light vans sold in 2025 shall be zero-emission vehicles.
Sweden	2030	Climate Policy Action Plan - Facts	Starting in 2030 it will no longer be permitted to sell new gasoline and diesel cars. Sweden is pushing for a similar ban within the EU.
Denmark	2030/2035	Climate and Air Plan	After 2030, new gasoline and diesel cars will no longer be sold in Denmark, and new PHEVs after 2035.
Iceland	2030	Climate Action Plan 2018–2030	New registration of diesel and gasoline cars will be unlawful after 2030. Exceptions, such as for remote areas, will be considered.
Ireland	2030	Climate Action Plan 2019	Ban of the sale of new fossil fuel cars from 2030 onward.
Netherlands	2030	Climate Agreement	New passenger cars will be emissions-free by 2030 at the latest.
Scotland	2032	Climate Change Plan	Scotland will phase out the need to buy gasoline and diesel cars and vans by 2032.
United Kingdom	2035	PrimeMinister Boris Johnson	To end the sale of new conventional gasoline and diesel cars and vans including PHEVs and HEVs by 2035.
France	2040	Mobility Guidance Law	To end of the sale of new passenger cars and light commercial vehicles using fossil fuels by 2040.
Spain	2040	Draft Law on Climate Change and Energy Transition	Goals are set for minimum shares of electric vehicles of total passenger cars sold, to reach 100% by 2040.

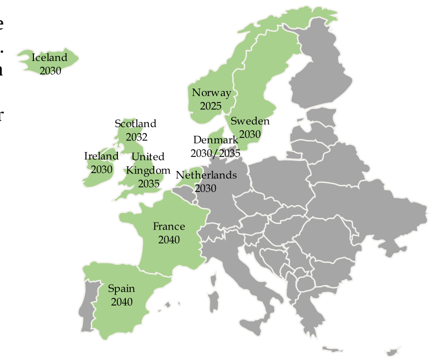

and easily expandable in a modular fashion.

Several studies have thoroughly analysed the energy impacts of single components, such as [12, 13 and 14]. Others take into account only a specific architecture and do not refer to nor evaluate its system with an existing car, such as [15] or [16].

Some authors compare different configurations, i.e. [17, 18 and 19], and calculate the overall consumed energy, but lack resolution at part-level. This work aims to join these two principles with a holistic model including part-level detail with full-system relevance and applicability.

There are some authors, i.e. [20], that study component-to-component energy consumption of the car by employing experimental data, but only for a certain configuration.

By contrast, other articles calculate energy management under different standard drive cycles, i.e. [21, 22, 23] or using data from real vehicles, such as [24] or [25]. However, not all parts are reflected individually or only one drive cycle is examined, for instance in [26].

Few other authors consider all components and their losses separately for a different ICE, electric motor, and type of vehicle, unfortunately not all configurations are included. It is the case, for example, of [27].

Besides, this paper provides a calculation methodology that includes vehicles of category L6e (light quadricycle) and L7e (heavy quadricycle), according to [28]. These vehicles are becoming increasingly important in urban mobility.

Current literature about quadricycles deals with fixed vehicle configurations ([29, 30, 31]) or calculations that are based on other parameters (for example [32] uses battery power consumption, driver comfort temperature, and travel time) or is focused on a single vehicle component (in [33] only studies of electric motors are included).

There are some existing optimization algorithms that have been applied in several studies on the defined optimal design issue. According to previous works like [34], existing optimization algorithms for EV, (P)HEV, and FCV technologies can be classified into three main types and sub-types of design optimization algorithms (see Fig. 1).

Rule-based strategies refer to a group of simple algorithms that are developed based on the operation modes of energy sources. It is used in a wide variety of research studies. For example [35], develops a consumption minimization strategy for series HEVs. In [36], the energy economy of plug-in hybrid electric vehicles (PHEVs) in the New European Driving Cycle (NEDC) is studied.

Nevertheless, global optimization-based strategies aim to achieve the best performance by minimizing the predefined objective functions. One of them is dynamic programming (DP). In [37], a global energy management optimization method for a HEV is provided, using DP in the world harmonized light-duty vehicle test procedure (WLTP). A methodology to improve fuel efficiency in parallel HEV is presented in [38], while ensuring good drivability and traffic efficiency. In [39], range is improved through the optimization of the ratio of energy provided by the fuel cell (FC) and battery in FCV.

Fewer literature is available for learning-based strategies. For example, in [40], cost minimization is formulated, including fuel consumption cost, the electricity cost of battery charging/discharging, and the equivalent cost of battery degradation. In [41], a PHEV bus is evaluated through a neural network approach to improve fuel economy in the NEDC and WLTP. In [42], a learning-based strategy is used to study fuel economy for PHEV.

Some literature combines or compares these design optimization algorithms to check its efficiency and viability. For example, in [43], a neural network strategy is applied to predict the future short-term velocity; meanwhile, DP is applied to calculate the optimal energy distribution at each step. In [44], three optimization algorithms (DIRECT, simulated annealing (SA), and genetic algorithm (GA)) are compared to optimize 6 design variables of a parallel HEV in a drive cycle composed of city (FTP-75 cycle) and highway driving (highway fuel economy test (HWFET) cycle).

On average, the GA method gives more accurate results for modal properties than other methods [45]. GA presents an intelligent exploitation of a random search to solve multi-objective

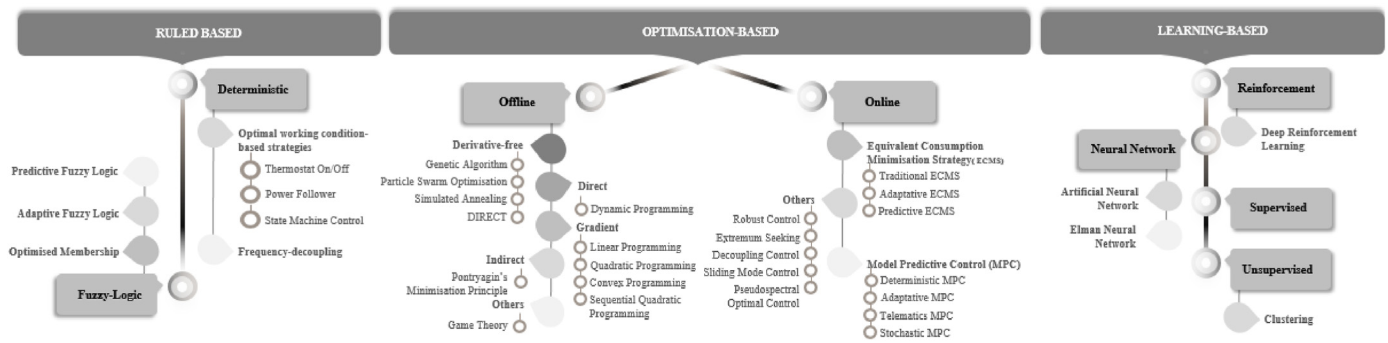

Fig. 1. Classification of existing optimization algorithms.

optimization problems. Despite being randomized, GAs use historical knowledge to direct the search into the region of better performance within the search space [46].

Due to these advantages, a GA was chosen as the optimization algorithm for seeking the best ESS and electric motor configuration for a given vehicle category and configuration. Likewise, it is intended to present a process that has not yet been tackled in the way outlined in this paper.

1.2. Contributions of the work

This paper attempts to make the following contributions and improvements to the state-of-the-art:

- This work presents a standardized operating system and hardware abstraction layer for application in the automotive sector.
- The proposed methodology is a simple, expandable, and highly accurate mathematical procedure. Its accuracy and reliability are verified under multi-pattern driving cycles. Moreover, the effectiveness of the procedure based on a GA is validated through performance comparisons with benchmarks in multiple case studies based on real vehicles. It is a transversal method including 4-wheeled EV, series (P)HEV, parallel (P)HEV, series-parallel (P)HEV (with one and three clutches structure), and FCV designs. It considers a variety of vehicle categories (L6e or Light quadricycles, L7e or Heavy quadricycles, M_1 vehicles or passenger cars, N_1 vehicles or motor vehicles for the carriage of a maximum mass of 3.5 tonnes and LSV [speed not more than 40 km/h and gross vehicle weight less than 1361 kg] [see more details in Section 2.1 *Input Data*]). With a single tool, results with different architectures/configurations or design criteria, or categories can be compared.
- This flexible method can be easily extended for different technologies of batteries and electric motors, different standard or customised drive cycles, etc. The computer program or application can be further extended with other vehicle parts and configurations in future works.
- The obtained results can be personalized by the user depending the selected criteria (costs, weight, and volume of different components).
- This methodology presents an excellent opportunity for creating a mobile application to improve the communication and business between several companies or suppliers and original equipment manufacturers (OEMs).

2. Methodology description and system modelling

This paper presents a methodology for designing and sizing electric motors and ESS for vehicles with different grades of electrification, focused on electric motors and ESS. A mathematical tool has been designed with the use of an optimization program.

Initially, the desired range, specifications, and architecture of the vehicle must be known, as well as the driving cycle (time and speed) as shown in the diagram in Fig. 2.

With all requisite data gathered, the flowchart of the iterative process of the GA is constructed as shown in Fig. 3.

In the following sections each of the phases of the flowchart in Fig. 3 will be described in more detail.

2.1. Input data

To begin, all the data to be entered in the system shall be defined.

A. Desired Range

The user should introduce the desired range in km to help the system design and dimension the vehicle and give the correct and desired result.

B. Vehicle Configuration

As discussed, the calculation-optimization system considers several topologies for EV, (series, parallel, and series-parallel) (P)HEV, and FCV, according to the following description. All of them are described in Fig. 4.

C. Vehicle Category

The described methodology is presented specifically for light-duty 4-wheeled for each of the named configurations within the categories L6e, L7e, M_1, N_1, and LSV defined in Figs. 6–10 [47–49].

D. Vehicle Specifications

To obtain results specific for a certain vehicle, some

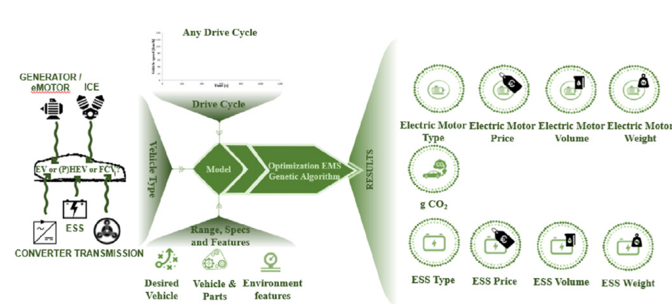

Fig. 2. Methodology description.

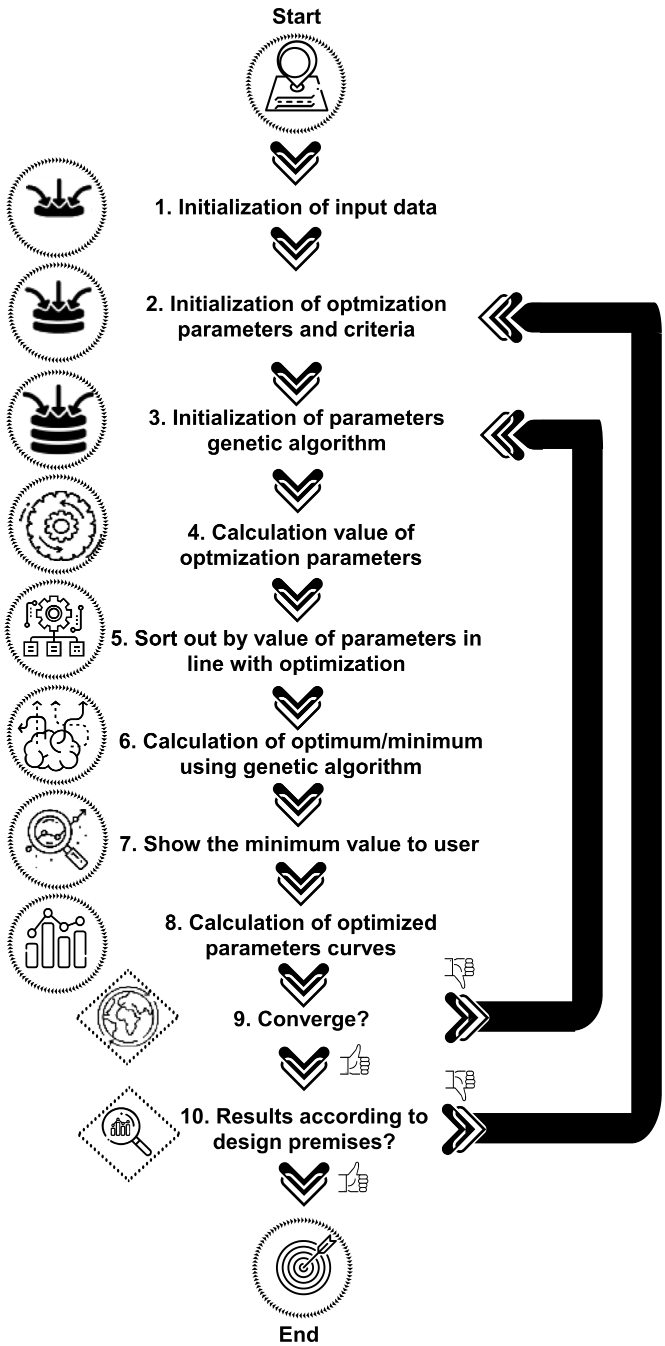

Fig. 3. Flowchart of the iterative process of the GA optimization.

specifications must be provided to the system. These include the traction shaft wheel type to calculate dynamic radius, weight, aerodynamic coefficients (drag coefficient and frontal area), transmission gear ratios, and ESS characteristics. Moreover, some features from the environment must be taken into account, e.g. air density and angle of slope.

E. Drive Cycle.

Different results will be obtained according to the provided drive cycle on the system. Both official (e.g. WLTP, environmental protection agency (EPA) cycle, NEDC, Japan cycle'08 (JC08), etc.) and customised drive cycles can be employed, demonstrating a flexible and expandable procedure.

A drive cycle is characterized by the vehicle speed in rpm (revolutions per minute), mph (miles per hour) or km/h (kilometres per hour) and time in s.

2.2. Basic Formulation

A Vehicle Dynamics

Basic principles of vehicle dynamics should be taken into account to describe automobile performance and the mathematical tool.

Longitudinal dynamics of the total running resistance (F_T) of an automobile are defined in (1) and represented in Fig. 5.

$$F_T = F_{In} + F_{Ro} + F_L + F_{si} \tag{1}$$

where F_{In} represents the inertia, F_{Ro} is rolling resistance, F_L is drag resistance and F_{Si} is climbing resistance.

Power (P) or necessary acceleration power is equal to the resistance power and any power losses:

$$P = F_T \cdot v/\eta \tag{2}$$

where η combines the power losses of the vehicle parts. In the present research it is expressed as the efficiency of each component of the car and will be discussed later in this paper.

The following equation is necessary to calculate the consumed energy to move the vehicle (E) as an integration of power at the ESS terminals:

$$E = \int_{traction} P_{out}(t)dt + \int_{braking} P_{in}(t)dt \tag{3}$$

where t is the drive cycle time in s. The first part of the formula calculates the energy invested in traction for the car. The second part calculates the energy recovered from regenerative braking by operating the motor drive as a generator and restoring energy to the batteries.

Given the growing importance of the greenhouse effect of vehicle emissions, some initiatives have been launched in the form of laws. For example, in Europe from 2020, OEMs begin to be fined for manufacturing vehicles that exceed 95 g CO_2/km on average. Electric vehicles do not emit CO_2, but ICE motors and the energy sources necessary to produce the electricity of the analysed vehicles do. So, these emissions have been included in the calculations made in this work. For that purpose, the calculated energy in (3) is necessary together with the composition of the energy sources.

$$g\ CO_2 = E \cdot \sum_{n}^{i} \%_{fuel} \cdot SCV \tag{4}$$

where SCV is the specific calorific value of the fuel in Wh or J per weight unit.

B. Efficiency Calculation Data

To determine energy distribution in a vehicle, the value of efficiency (η in (2)) of each component shown in Fig. 4 is essential. Different aspects must be analysed given that this value is not identical for every vehicle. This statement is confirmed in this paper.

First of all, a vehicle needs energy to be moved, that is the mission of an ESS. Batteries are the most common used in electric, hybrid, and plug-in hybrid vehicles. In the case of a BEV, energy comes from

EV	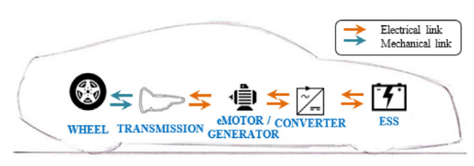	Pure EV drivetrains are essentially composed of an ESS, a converter (operating as an inverter in connection between the ESS (direct current (DC)) and electric motor (alternating current (AC)) or as a rectifier in connection between the generator (AC) and ESS (DC)), a traction machine (an electric motor that works as a generator in case of regenerative braking) and a mechanical transmission. This is, for example, the case of the Tesla X P90D, Tesla S 85, Nissan Leaf, Renault Zoe, Volkswagen e-Up! and e-Golf, BMW i3, and Chevrolet Spark. The included categories are L6e, L7e, M_1, N_1, and LSV.
Parallel (P)HEV	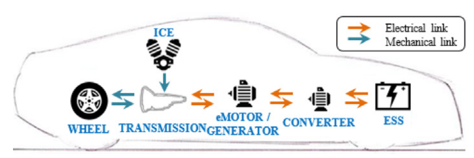	In (P)HEV, an ICE is coupled to deliver additional power to vehicle. The most common fuels are gasoline and Diesel and are the only ones considered in this research. In the case of parallel (P)HEV, both the ICE and electric motor can work together or separately to provide power to the transmission of the vehicle. This is, for example, the case of the Ford C-MAX Energi, Audi A3 Sportback etron, Volkswagen Golf GTE, Volkswagen XL1, and BMW i8. The included categories are M_1 and N_1.
Series (P)HEV	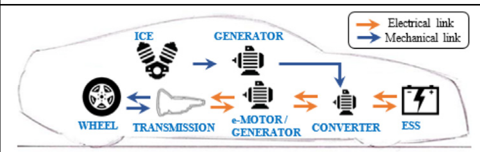	In series HEV, an ICE is coupled to a generator to deliver additional electric power to the vehicle. The rest of the structure is similar to the EV architecture. This is, for example, the case of the BMW i3. The included categories are M_1 and N_1.
Series-parallel (P)HEV	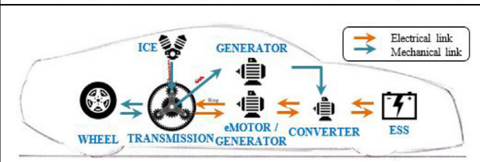	In a Series-Parallel HEV, there is an ICE connected to the transmission (like parallel structure) and also an extra generator linked to the converter (like series structure) to provide electric energy. This is, for example, the case of the Toyota Prius and Chevrolet Volt. The included categories are M_1 and N_1. This paper includes the calculations for the mechanical structure of the Toyota Prius and the Chevrolet Volt. A major difference between these two designs lies in the fact that the Prius does not use any clutch and the Volt has three clutches.
FCV	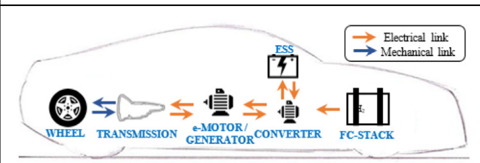	Taking into account new portable energy sources, FC are taking advantage regarding automotive applications given to their benefits and potential. An additional battery is necessary to accumulate the energy provided by regenerative breaking, since FC, in contrast to batteries, allows only unidirectional power flow. This is, for example, the case of Toyota Mirai, Honda Clarity FC, Hyundai ix35 / Tucson FCEV and Mercedes Benz GLC F-Cell. The included categories are M_1 and N_1.

Fig. 4. Vehicle Configuration.

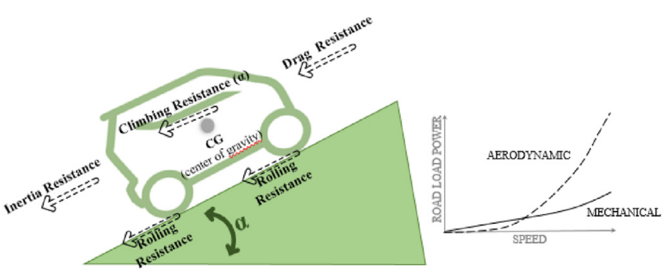

Fig. 5. Vehicle longitudinal dynamics.

the electric grid. As said before, the efficiency of the charging process is not considered. The aim of this paper is to analyse tank to wheel energy, that is to say, the energy needed to produce, transport, and distribute fuel is not included in this research. This paper includes analysis of nickel-metal hydride (NiMH) and lithium-ion (Li-ion) technology. The available documentation corroborates that NiMH batteries have different efficiency than that of Li-ion. The efficiency value stated by [50] for NiMH batteries is about 90%, however, in [51] is indicated that Li-ion batteries have an efficiency between 88.9% and 96.3% depending on cell capacity and energy and power density.

The element that enables the mechanical movement of a car is the electric motor. This paper includes those most often employed in EV: induction motors, permanent magnet motors, and hybrid synchronous electric motors (with permanent magnets and reluctance effect). The efficiency is calculated for each drive cycle and motor type through its efficiency map of torque versus motor speed. Different real efficiency maps that should be considered for the calculation are, in particular:

a. For surfaced permanent magnet (SPM), the map of Nissan Leaf;
b. For interior permanent magnet (IPM), the map of Toyota Prius 3rd generation;
c. For hybrid synchronous electric motor, the map of BMW (Bayerische Motoren Werke) i8; and
d. For induction motor (IM) the one showed in [52].

Consistent with the obtained results for these electric motors, efficiencies are between 85% and 91% as stated in [53,54].

By contrast, according to [27], the efficiency of a tractive machine working as a generator is lower than when the device actuates as an electric motor. Specifically, this efficiency is 5% lower.

In the case of (P)HEV, the combustion engine must also be considered. References [55,56] demonstrate the minimal energy losses for an ICE to be 65% and [27] helps to distinguish the efficiencies for different car and engine dimensions (small cars, large cars, and SUVs (sport utility vehicles)).

Batteries operate with DC and electric motors work with AC. To make the connection possible, converters are necessary and they are considered to have an efficiency of 95% according to [57] when they work as an inverter (DC → AC) or as a rectifier (AC → DC).

To transfer motor torque to the wheels, a drive chain system must also be taken into consideration. The general efficiency value determined by [57] is 90%. However, it should be noted that this can vary depending on vehicle dimension as remarked in [27]. Additionally, according to the obtained results, it is important to take into account that complex batteries suffer from higher losses. In this work, the most complex, i.e., the largest analysed, is the Tesla X P90D and Tesla S 85 battery pack, comprised of 7104 Panasonic NCR18650 cylindrical batteries in a 96s74p structure.

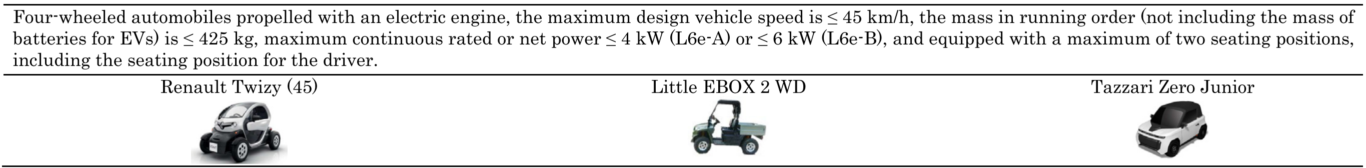

Fig. 6. L6e - Light quadricycle.

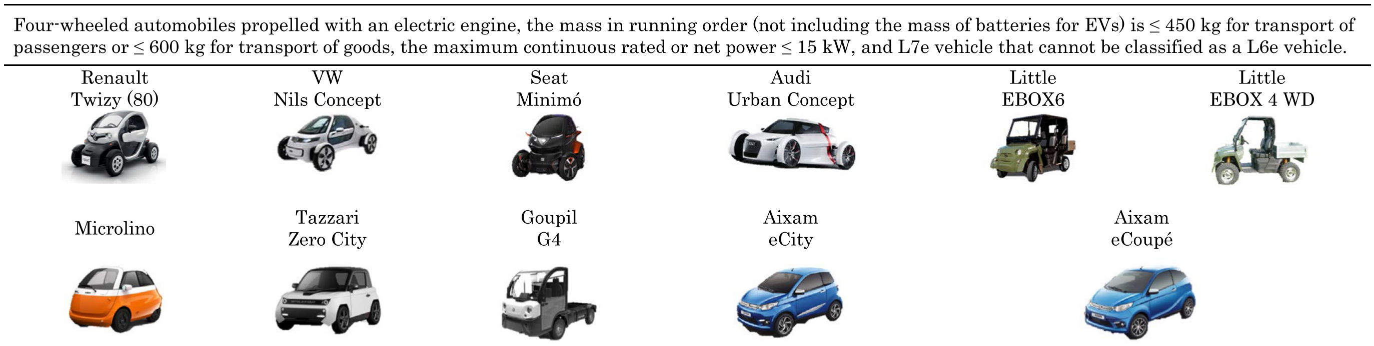

Fig. 7. L7e - Heavy quadricycle.

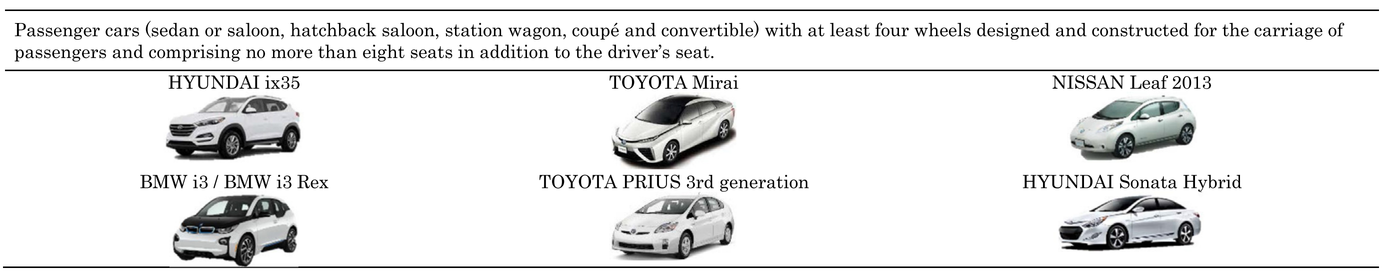

Fig. 8. N_1 vehicles.

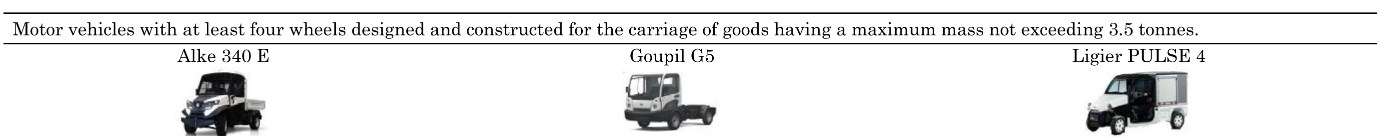

Fig. 9. M_1 vehicles.

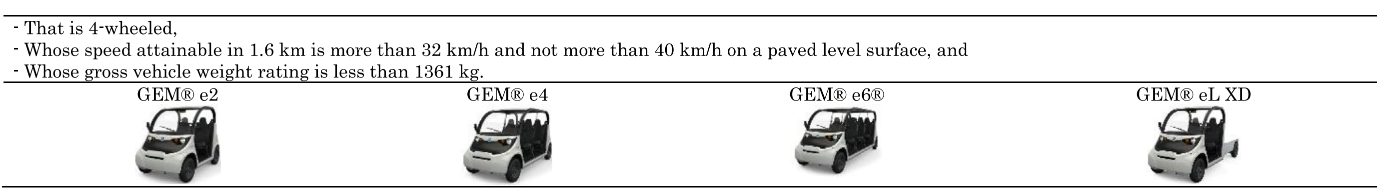

Fig. 10. LSV - Low-speed vehicle.

Moreover, in line with the consulted literature, other factors have to be considered, for example, parasitic losses including electrical losses, the electric motor generating limit (motor rating dependent), vehicle stability considerations, battery state conditions such as fully charged state or high temperature, very low speed/low voltage restrictions (where power electronics cannot function properly) and further vehicle drivability considerations [58]. All these additional aspects suppose losses of 2.5% of the employed energy [58].

B CO_2 Calculation

Due to the growing importance that CO_2 production has taken from the environmental point of view, the grams of CO_2 produced to generate the energy necessary to cover the desired range has been considered relevant in this paper. Table 2 has been built using literature data [59,60] to show the grams of CO_2 emitted according to the energy source and its place of origin. The calculations are carried out using (4). In the case of the Atkinson and Diesel ICE, the

Table 2
Electricity and CO_2 generation by source.

	Europe		United States		World		
	Electricity Generation [TWh]	[%]	Electricity Generation [TWh]	[%]	Electricity Generation [TWh]	[%]	g CO_2/kWh
Coal	1083	34	1559	44	9914	44	451
Oil	81	3	37	1	986	4	238
Natural gas	1057	33	1209	34	5170	23	210
Hydro	276	9	292	8	4152	18	8
Nuclear	118	4	100	3	402	2	10
Wind	209	7	230	6	950	4	14
Solar	113	4	50	1	323	1	57
Biofuels&waste	259	8	81	2	726	3	70

values of 266 g CO_2/kWh and 267 g CO_2/kWh are taken respectively. In the case of the NEDC, WLTC, and ECE-15 drive cycles, the program calculates the emissions from the data from Europe.

For the EPA drive cycle, the program calculates emissions from United States data. And, in relation to the "World" table, in any case the data is used to calculate the grams of CO_2 regardless of the drive cycle.

According to Table 2, electric vehicles need to be charged using renewable energy-based electricity such as photovoltaic solar panels, hydro or wind in order to prevent and minimize such its environmental adverse effect [61].

2.3. Definition and calculation of optimization parameters and proportion criteria

The three parameters to be calculated in the GA are the costs, volumes, and weights of the ESS and the electric motor.

It is first necessary to choose which parameter or parameters should be considered. Equations for the parameters value calculation are described below.

$$Cost_{ESS} = E \cdot Price_{ESS\ Energy} \quad (5)$$

where $Cost_{ESS}$ is the calculated cost of the studied ESS in € (or any other monetary unit), E is defined in (3), and $Price_{ESS\ Energy}$ is the price of the ESS technology in €/kWh.

$$Volume_{ESS} = E/_{\rho_{ESS\ Year}} \quad (6)$$

where $Volume_{ESS}$ is the calculated volume of the studied ESS in l (litres) or m^3 and $\rho_{ESS\ Year}$ is the volumetric energy density of the ESS technology in Wh/l or Wh/m^3.

$$Weight_{ESS} = E/_{\rho_{ESS\ Year}} \quad (7)$$

where $Weight_{ESS}$ is the calculated weight of the studied ESS in kg and $\rho_{ESS\ Year}$ is the gravimetric energy density of the ESS technology in Wh/kg.

$$Cost_{eMotor} = P \cdot Price_{eMotor\ Energy} \quad (8)$$

where $Cost_{eMotor}$ is the calculated cost of the studied electric motor in € (or any other monetary unit), P is defined in (2), and $Price_{eMotor\ Energy}$ is the price of the motor in €/kW.

$$Volume_{eMotor} = Torque/_{\rho_{eMotor\ Year}} \quad (9)$$

where $Volume_{eMotor}$ is the calculated volume of the studied electric motor in l (litres) or m^3, $Torque$ is the torque of the cycle in N·m, and $\rho_{eMotor\ Year}$ is the volumetric torque density of the electric motor technology in Nm/l or Nm/m^3.

$$Weight_{eMotor} = Torque/_{\rho_{eMotor\ Year}} \quad (10)$$

where $Weight_{eMotor}$ is the calculated weight of the studied electric motor in kg and $\rho_{eMotor\ Year}$ is the gravimetric torque density regarding the electric motor technology in Nm/kg.

Proportion criteria are defined according to the proportion of the parameters as shown in Table 3, that is, users must indicate which parameter should be prioritized.

Table 3
Proportion criteria.

Proportion Cost	Proportion Volume	Proportion Weight
x	y	z

where

$$x + y + z = 1 \quad (11)$$

2.4. Parameters of optimization algorithm (genetic algorithm)

As mentioned before, the chosen method to optimize the drivetrain design is a GA, an evolutionary algorithm and artificial intelligence method. It is chosen as one of the most efficient algorithms [62] and given its strengths and advantages [46,57] (GA is an adaptive, multi-objective, and multi-variable algorithm; it is a global search method and offers global solutions and does not require a priori knowledge of driving cycle).

According to the view of evolution, GAs follow a clear process optimization, working on a population which is composed of several individuals (or possible, randomly generated solutions). An individual is made up of chromosomes, which contain part of the genes or information and decision variables (see Table 4). This population is subjected to certain transformations and then to a selection process that favours the best; it is expected that the best

Table 4
Parameters to be used in the GA.

Chromosomes		
Type ESS:	Type EM:	Battery Cell Capacity
- NCA	- SPM	Energy cost
- LCO	- IPM	Energy density
- NMC	- IM	Power cost
- LMO	- Hybrid	Torque density
- LFP		
- LTO		
- NiMH		
- FC		
Genes	Genes	

individual in the population is close to the desired solution [63–65].

In Table 4, the parameters to be used in the GA are shown as input data to be optimized and to find the right results according to the user requirement/s.

Within the population, each individual is distinguished according to their aptitude or fitness (ranking according to the objective function), which is obtained using some measures according to the problem to be solved. In this case, fitness prioritizes the minimum value of the cost, volume and/or weight of both the battery and electric motor.

A new generation is obtained by using the selection operator. According to the evolutionary theory, the best individuals have the highest probability to join the next population. The next step is crossover, which makes a certain number of individual pairs, selected randomly, exchange some of their genes with each other. The resulting genes of the individuals will of course behave differently in the next population, thus yielding new individuals. After crossover, mutation takes place, once again based on a random selection of individuals, which modifies elements in the chromosomes. The purpose of the mutation operator is to maintain diversity within the population and inhibit premature convergence [46].

Initial values for the chromosomes and genes are needed in order to start the calculations. The year 2019 has been taken as the time reference for the data. The used value for crossover probability is 0.9 and the mutation probability 0.025. Crossover is allowed with the battery parameters or the electric parameters but never with a mixture of them. The mutation is defined to take place only in one chromosome.

The period required to conceive a vehicle is considered to be 4 years. Therefore, the program is designed to take into account that the results should be calculated over a horizon of this period.

To continue with the calculations, it is necessary to characterize the ESS and electric motors technologies according to Table 4.

The ESS and electric motor type must be entered by the user/designer.

As for the energy cost, the information found in [66–68] shows that there is no fixed value and it decreases with time. All the data have been contrasted to construct Fig. 11 with the evolution of the energy cost for the different ESS technologies taken into account in Table 4.

In order to enter the data in the algorithm, it is also necessary to establish an annual relationship between the energy density of the year of calculation and the time reference.

Through a thorough study of references like [69–71], the values in Table 5 have been established as reference values.

Likewise, the literature shows that there is an evolution of technology in a way that improves over time. With the tests carried out in the procedure, it has been concluded that the relationships between densities are those reflected in (12) and (13).

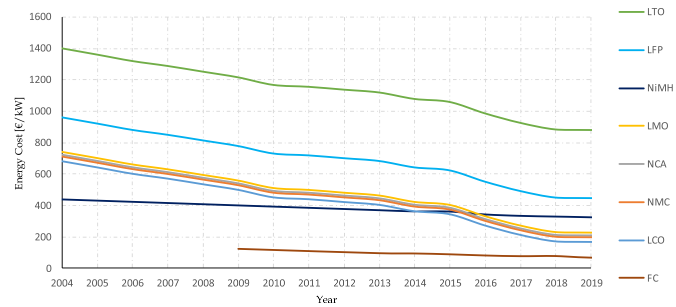

Fig. 11. Evolution of €/kWh in ESS technologies.

Table 5
Reference values of densities in the reference year (2019).

	FC	NCA	LCO	NMC	LMO	LFP	LTO	NiMH
Wh/l	1600	525	370	515	315	210	100	250
Wh/kg	1100	140	141	144	115	85	60	80

$$\rho_{Vol\ ESS\ Year} = \rho_{Vol\ ESS\ RefYear} \cdot (1 - 0.014)^{(RefYear - Year)} \qquad (12)$$

where $\rho_{Vol\ ESS\ Year}$ is the volumetric energy density of the ESS technology in Wh/l and $\rho_{Vol\ ESS\ RefYear}$ is selected from the values in Table 5.

$$\rho_{Grav\ ESS\ Year} = \rho_{Grav\ ESS\ RefYear} \cdot (1 - 0.058)^{(RefYear - Year)} \qquad (13)$$

where $\rho_{Grav\ ESS\ Year}$ is the gravimetric energy density of the ESS technology in Wh/kg and $\rho_{Grav\ ESS\ RefYear}$ is selected from the values in Table 5.

In relation to electric motors and contrasting data from different sources, i.e. [72–74], prices depend on their technology, power, supplier, country of manufacture, and purchase volume, so they cannot be taken into account as a reference. Therefore, this work will focus on the benchmarking carried out on 81 real vehicles and on the annual variation of the costs of an electric motor according to [75]. In any case, the methodology described in this paper allows the user to enter the exact data of the genes so that the calculations are more accurate.

Table 6 shows the data used for the calculations related to the electric motors. The basic values in the table have been extracted from a thorough analysis of references [76–78].

Table 7 presents data obtained from the benchmarking of 81 vehicles available in the market. It can be concluded that the electric motor has different characteristics depending on the configuration of a vehicle, so it is considered important for characterization.

BEV micromobility includes vehicles of the following categories: L6e or Light quadricycle, L7e or Heavy quadricycle, and LSV or low-speed vehicle.

According to [75], the price of an electric motor of an IPM is a function of its power (see Table 8).

Using these data, the evolution of the motor prices are

Table 6
Reference values of prices and densities in the reference year (2019).

	SPM	IPM	IM	**Hybrid** (permanent magnets + reluctance effect)
€/kW	51.6	47.6	12.7	9.1
Nm/l	21.9	17.5	4.2	11.5
Nm/kg	11.2	10.9	7.4	9.4

Table 7
Benchmarking of mean Power.

Vehicle Type	Power [kW]
BEV	156
PHEV S	125
FCV	118
PHEV S–P	80
PHEV P	67
HEV P	50
HEV S–P	45
BEV micromobility	14

Table 8
Cost of electric motor.

Year	Motor Cost
2012	50 € + 8 €· [kW]
2020	40 € + 6.4 €· [kW]
2030	32 € + 5.1 €· [kW]

calculated as a function of time and presented in Table 9.

Thanks to the tests carried out with the developed optimizing GA, it is concluded that the relationship between the density of the calculated year and the reference year is that reflected in (14).

$$\rho_{eMotor\ Year} = \rho_{eMotor\ RefYear} \cdot (1 - 0.001 \cdot Torque_{max})^{(RefYear - Year)} \tag{14}$$

where $\rho_{eMotor\ Year}$ is the density of torque of the electric motor technology in Nm/l and Nm/kg, $\rho_{eMotor\ RefYear}$ are the values showed in Table 6 and $Torque_{max}$ is the maximum value of the torque in the selected drive cycle.

Given that in Section 3. *Results* it is verified that this methodology works with real vehicles that are already on the market, the application will also be considered useful for future vehicles.

As already mentioned in the paper, the design period of a vehicle is considered to be 4 years, that is, with the presented methodology it is possible to calculate and predict the specifications of a vehicle that could be manufactured with the date of start of production in 2023. If the reference data showed in Fig. 11, Tables 5 and 6 are updated, this methodology can be used for any start of production time.

Therefore, in relation to the evolution of the price of ESS, if the same scheme of calculations and procedure is followed, the results of Fig. 12 and Table 10 are obtained.

Based on (12) and (13), the calculation formulas to be used are achieved, obtaining (15) and (16).

$$\rho_{Vol\ ESS\ 2023} = \rho_{Vol\ ESS\ 2019} \Big/ (1 - 0.014)^4 \tag{15}$$

$$\rho_{Grav\ ESS\ 2023} = \rho_{Grav\ ESS\ 2019} \Big/ (1 - 0.058)^4 \tag{16}$$

Table 9
Evolution of the price of an electric motor in comparison with 2019

Year	Difference in price with 2019 [%]	Year	Difference in price with 2019 [%]
2003	27.4	2012	14.2
2004	26.1	2013	12.4
2005	24.8	2014	10.5
2006	23.5	2015	8.6
2007	22.0	2016	6.6
2008	20.6	2017	4.5
2009	19.1	2018	2.3
2010	17.5	2019	0
2011	15.9		

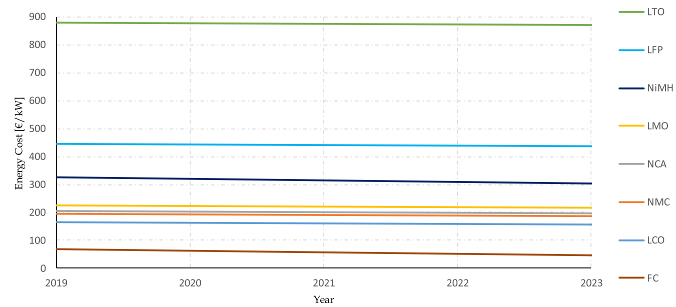

Fig. 12. Evolution of €/kWh in ESS technologies in 4 years.

Table 10
Evolution of ESS prices in 4 years.

Type ESS	Difference in price in 4 years [%]
NCA	- 4.1
LCO	- 5.0
NMC	- 4.3
LMO	- 3.7
LFP	- 1.9
LTO	- 1.0
NiMH	- 6.8
Fuel Cell	- 33.3

In the same way, the previously presented assumptions have been used to obtain the result shown in Table 11. The price trend shown in Table 9 together with the values of Table 6 are used to project the expected electric motor price in 2023.

Table 11
Evolution of the price of an electric motor in 4 years.

Year	2019	2023
Difference in price in 4 years [%]	0,0	- 9.4

Based on (14), the calculation formula to be used is found, obtaining (17).

$$\rho_{eMotor\ 2023} = \rho_{eMotor\ 2019} \Big/ (1 - 0,001 \cdot Torque_{max})^4 \tag{17}$$

The optimization algorithm is viably executed by introducing the information detailed in the present section.

Using input data from any year, this methodology can be used for the design of a future vehicle of any of the described configurations and categories.

2.5. Calculation of optimized parameters curves

Once all the parameters have been calculated, they are shown on a graph to check whether the results actually converge to an optimal solution.

In Figs. 13–19, results obtained from a simulation process for the criteria in Table 12 are shown.

In Figs. 13 and 15, the evolution with each iteration of cost and weight, respectively, can be checked. The rest of the graphs are the

Table 12
Proportion criteria.

Proportion Cost	Proportion Volume	Proportion Weight
0.25	0	0.75

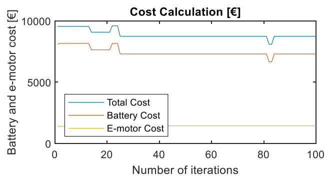

Fig. 13. Chart for cost calculation.

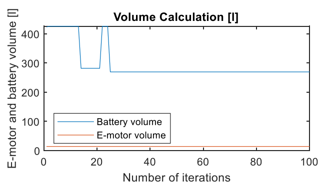

Fig. 14. Chart for volume calculation.

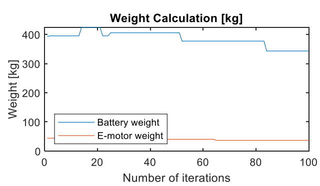

Fig. 15. Chart for weight calculation.

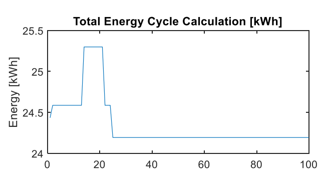

Fig. 16. Chart for total energy cycle calculation.

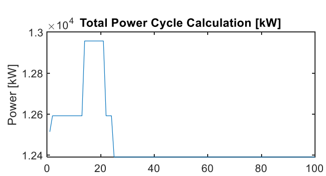

Fig. 17. Chart for total power cycle calculation.

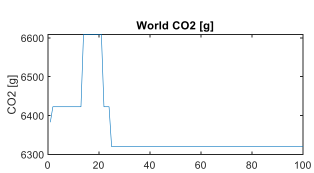

Fig. 18. Chart for CO_2 calculation (world hypothesis).

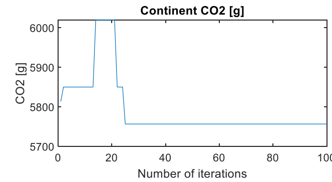

Fig. 19. Chart for CO_2 calculation (continent hypothesis).

result of the calculations of the imposed criteria, including Fig. 14, even though, in this case, the value of the volume criterion is zero.

2.6. Scope of calculation and results

Based on the relationship between vehicle weight and ESS weight in a benchmarking of 81 real vehicles, a limit is set to determine whether a result of the program calculation is feasible or not. Prior literature [70] establishes that an ESS represents 20–25% of the total weight of an EV. Since there are many other vehicle configurations and the technology has evolved since that paper, a market study has been developed in this paper and the conclusions are shown in Table 13.

If all design premises, input data, optimization parameters, and criteria do not result in a realistic design limited by the data in Table 13, then the initial conditions must be revised.

Table 13
Limits on ESS weight vs vehicle ratio for all configurations.

	BEV	BEV Micromobility	series (P)HEV	parallel (P)HEV	series-parallel (P)HEV	FCV
Relation ESS and total weight [%]	30	25	20	17	17	5

3. Results

The aim of this paper is to find the minimum value of the cost, volume, and/or weight of both the battery and electric motor for the given input data specified by the designer. The presented mathematical method is capable of calculating the most economic (minimum cost), the smallest (minimum volume), the lightest (minimum weight), or some other optimized option based on the combination of these three factors.

To begin the calculations, the efficiency of the vehicle must be determined.

3.1. Efficiency calculation results

All the theory stated in the previous section is employed to look for the efficiency of some vehicles.

In Tables 14–16 results obtained are shown.

It can be checked in Fig. 20 that those vehicles with the highest efficiency are pure electric vehicles, followed by hybrid vehicles and, finally, the lowest value corresponds to FCVs.

Table 14
Total efficiency of M_1 (P)HEV and FCV.

	Vehicle	Year	Cycle	Total Official Efficiency [%]	Total Calculated Efficiency [%]	ε [%]
M_1 Series (P)HEV	BMW i3 Rex	2013	NEDC	61.2	57.9	5.7
M_1 Ser.-par. (P)HEV	TOYOTA PRIUS (3rd gen)	2009	NEDC	46.2	46.5	0.6
	CHEVY VOLT	2016	EPA	45.2	45.0	0.4
M_1 Parallel (P)HEV	HYUNDAI Sonata Hybrid	2011	NEDC	46.7	41.6	5.6
	FORD C-MAX ENERGI	2014	EPA	43.7	45.7	4.3
	AUDI A3 etron	2014	NEDC	51.2	47.2	8.6
	VW Golf GTE	2015	NEDC	51.1	47.2	8.2
	VW XL1	2013	NEDC	38.4	38.5	0.4
	BMW i8	2013	NEDC	41.6	39.8	4.5
M_1 FCV	TOYOTA MIRAI	2015	NEDC	34.1	35.0	2.5
			EPA	34.0	34.1	0.2
	HONDA CLARITY FC	2016	EPA	36.5	34.6	5.6
	HYUNDAI ix35/TUCSON FCEV	2013	NEDC	32.9	34.6	5.1
	MB GLC F-CELL	2017	NEDC	37.6	35.6	5.8

Table 15
Total efficiency of L6e, L7e and N_1 BEV.

	Vehicle	Year	Cycle	Total Official Efficiency [%]	Total Calculated Efficiency [%]	ε [%]
L6e BEV	Renault Twizy (45)	2018	ECE-15	58.1	59.2	1.9
	Little EBOX (2WD)	2013	25 km/h	70.7	67.3	5.0
L7e BEV	Renault Twizy (80)	2018	ECE-15	61.6	59.2	4.1
	Little EBOX 4WD	2013	25 km/h	63.5	65.1	2.4
	Little EBOX6 2WD	2013	25 km/h	68.3	66.6	2.6
	Little EBOX6 4WD	2013	25 km/h	67.9	65.1	4.3
	Aixam eCity	2019	ECE-15	60.2	60.1	0.2
	Aixam eCoupé	2019	ECE-15	60.2	60.1	0.2
	Audi Urban Concept	2011	NEDC	66.1	63.9	3.4
	VW Nils Concept	2011	NEDC	67.3	66.2	1.6
	Microlino	2019	ECE-15	62.3	62.5	0.3
N_1 BEV	MIA electric	2013	NEDC	56.9	59.8	4.8
	Tazzari Zero EM2 Space	2019	NEDC	55.1	58.2	5.3

Table 16
Total efficiency of N_1 BEV.

	Vehicle	Year	Cycle	Total Official Efficiency [%]	Total Calculated Efficiency [%]	ε [%]
N_1 BEV	TESLA S 85	2013	NEDC	62.7	60.9	2.9
		2013	EPA	63.3	61.7	2.7
	TESLA X S90D	2016	NEDC	64.6	61.1	5.7
		2016	EPA	66.0	62.4	5.8
	VOLKSWAGEN e-UP!	2013	NEDC	64.8	63.7	1.8
	VOLKSWAGEN e-GOLF	2015	NEDC	69.3	66.5	4.3
	BMW i3	2013	NEDC	64.0	62.0	3.3
	CHEVY SPARK	2015	EPA	61.3	64.1	4.3
	NISSAN LEAF	2013	NEDC	70.4	67.2	4.9
		2017		71.2	66.8	6.5

3.2. Genetic algorithm calculation results

In order to verify that the established hypothesis and calculations are correct, technical characteristics of a vehicle have been taken as input data for each configuration considered in this paper. These vehicles are: a pure electric vehicle, the Nissan Leaf and the BMW i3 (both models of 2013); a plug-in hybrid series vehicle, the 2013 BMW i3 Rex; a parallel hybrid vehicle, the 2011 Hyundai Sonata; a series-parallel hybrid vehicle, the 2009 Toyota Prius (3rd generation); a FCV, the 2015 Toyota Mirai; and two pure electric vehicles belonging to the micromobility group, the 2018 Renault Twizy 80 and 45.

In Table 17 some of these specifications are shown.

The results shown in Table 18 have been obtained using the described method and numeric data taken from meticulous analysis of the literature.

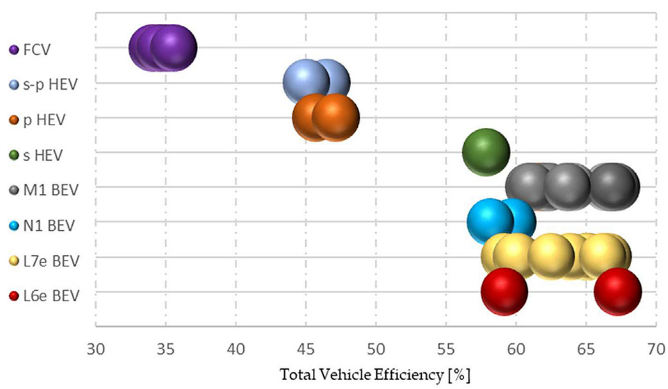

Fig. 20. Total vehicle efficiency for different vehicle configurations.

In Table 18, the real values of the weight and volume of the battery and/or FC and of the electric motor for each case are compared with those calculated through the methodology presented in this paper, taking into account the characteristics of the technology that are available, according to Table 4. Then, a GA looks for the best solution according to the conditions that have been imposed at the beginning such as desired range and other characteristics.

The proportion of cost, volume, and weight that are considered adequate according to the design criteria must also be defined, so that the GA returns the most appropriate type of battery (for non-FCV) and electric motor technology to use. In the case of FCV, the result is independent of the battery technology since, according to current know-how, its dimensions and economic value are negligible compared to the FC stack.

With the data indicated in Table 2 in Section 2.2 *Basic Formulation*, the presented procedure allows for calculating the amount of CO_2 formed from producing the electricity necessary to charge the batteries or produce H_2 for the fuel cells. This information also helps designers when deciding the structure of a vehicle if they cannot decide on the primary energy source from which electricity is obtained. The GA finds the best solution and the numeric values shown in Table 18 are obtained.

In the case of electric motors, it has not been possible to verify their price through existing literature.

Furthermore, in Table 18, the price of the Hyundai Sonata battery could not be verified because it is included in the vehicle's warranty, so its purchase is not possible.

It has been possible to validate, for all the vehicle configurations and categories presented in this paper, that the method works with excellent reliability given the low error values obtained (see column ε [%]).

As verified according to the results shown in Table 18, the method not only works for all vehicle architectures, but also for any drive cycle, for instance, in this case, in NEDC, ECE-15, and EPA.

It can also be seen from Table 18 that the most frequently used criteria by Asian OEMs (Nissan (in alliance with the French Renault), Hyundai, and Toyota) is to prioritize weight without taking volume into account at all. On the other hand, the German BMW gives more importance to volume and cost over weight.

In the case of the weight of the battery on the Nissan Leaf, the result is not so accurate, possibly because the composition of the cells is a blend of LMO and LNO cathodes. This study, because of the lack of the information from real cars, has not included mixed cathodes.

In the case of both Twizys, the results related to weight and price for electric motor are obviously incorrect. The validity of the method is demonstrated with all other results and, at the moment, there is no sufficient available body of data from L6e and L7e cars to compare the method with other models in the same category. For the rest of parameters studied, the method provides adequate agreement.

Regarding both versions of the BMW i3, the BEV and PHEV, it is demonstrated that the method works properly because the base vehicle is basically the same and the calculations show that the method agrees for different configurations as well.

For the case of the Toyota Prius 3rd generation (series-parallel HEV) and Hyundai Sonata (parallel HEV), it can also be observed that the results are close to reality with a maximum of 15% error. This is a very good result, taking into account that the used numbers are mean values of densities and prices due to the lack of real published data by the brands.

Results are even better for the case of the Toyota Mirai fuel cell, where the volume value is exactly the real one and the FC weight and volume have a 3 and 4% error respectively.

In Fig. 21 dispersion of the values of ε is plotted to show that the method, for the values that have been published, works with great effectiveness and efficiency. Only the values of the weight of the battery of Nissan Leaf and the weight of the electric motor of both Renault Twizys have not been accurately resolved for the reasons already indicated.

4. Conclusions

In this paper, a simple and flexible methodology has been presented. It allows to achieve, with a software based, non-linear, intelligent GA, the calculations of drivetrain parameters and carbon emissions for different vehicle configurations and drive cycles (standard or customised), according to criteria selected by the designer. The mathematical method is capable of calculating the most economic (minimum cost), the smallest (minimum volume), the lightest (minimum weight), or some other optimized option based on the combination of these three factors of both the battery and electric motor.

The presented methodology provides a high degree of flexibility in the design and sizing of ESS and electric motors, taking into account the whole vehicle.

A benchmarking of 81 vehicles available on the market has been taken into account, establishing a limit to determine whether a result of the calculation program is feasible or not based on all design assumptions, input data, optimization parameters, and criteria.

Despite common simplifications among all vehicle configurations, the results obtained are extraordinarily correct, despite the fact that some of the input data is the result of taking simple mean values from the literature.

A manufacturer or other entity interested in the methodology, with the exact numeric input data, can obtain even more accurate and exact results.

Table 17
Specifications Nissan Leaf (2013), Renault Twizy 80 and 45 (2018), BMW i3 and BMW i3 Rex (2013), Toyota Prius (2009), Hyundai Sonata Hybrid (2011) and Toyota Mirai (2015). Sources: [72] [79] [80] [81] [82] [83] [84] [85] [86] [87] [88] [89].

			Nissan Leaf BEV M_1	Renault Twizy 80 BEV L7e	Renault Twizy 45 BEV L6e	BMW i3 / BMW i3 Rex BEV M_1 / Series PHEV M_1	Toyota Prius Series-Paral.HEV M_1	Hyundai Sonata Paral. HEV M_1				Toyota Mirai FCV M_1
				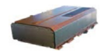								
									Fuel Cell Stack	Fuel		H_2
Battery	Cathode		LMO(NCA)	LMO	LMO	NMC	NiMH	LMO		Tank Capacity	[kg]	5 (700 bar)
	Configuration		96s2p	2s21p	2s21p	96s24p	168s1p	72s1p		Voltage	[V]	650
	Energy	[kWh]	24	6.1	6.1	21.8	1.3	1.4		Power	[kW]	114
	Weight	[kg]	294	98	98	233	41	35		Weight	[kg]	56
	Volume	[l]	494	69	69	211	48	47		Volume	[dm³]	37
Electric Motor												
	Type		IPM	IM	IM	hybrid (permanent magnets + reluctance effect)	IPM	IPM				
	Power	[kW]	80	13	4	125	60	30				
	Torque	[N·m]	280	57	33	250	207.44	205				
	Weight	[kg]	56	37	30	42	38	35				
	Volume	[l]	18	13	8	20	13	10				

Table 18
Final results for all vehicle configurations.

	Nissan Leaf BEV M_1			Renault Twizy 80 BEV L7e			Renault Twizy 45 BEV L6e			BMW i3 BEV M_1		
	Real	Calc	ε[%]	Real	Calc	ε[%]	Real	Calc	ε[%]	Real	Calc	ε[%]
Drive Cycle		NEDC			ECE-15			ECE-15			NEDC	
Type of Battery or FC	LMO+LNO	LMO	-	LMO	LMO	-	LMO	LMO	-	NMC	NMC	-
Volume Battery or FC [dm^3]	494	438	**11**	69	59	**14**	69	68	**1**	211	206	**2**
Weight Battery or FC [kg]	294	406	**38**	98	88	**10**	98	102	**4**	233	228	**2**
Price Battery or FC [€]	8448	8.399	**1**	2460	2337	**5**	2460	2843	**15**	6600	6164	**7**
Type of eMotor	IPM	IPM	-	IM	IM	-	IM	IM	-	IM	IM	-
Volume eMotor [dm^3]	18	14	**20**	13	11	**15**	8	7	**13**	20	21	**7**
Weight eMotor [kg]	55	44	**20**	37	7	**81**	30	4	**87**	42	45	**7**
Price eMotor [€]	-	1440	-	-	38	-	-	36	-	-	223	-
World g CO_2 [g CO_2/km range]		6608			1946			2237			5331	
Continent g CO_2 [g CO_2/km range]		6019			1772			2037			4856	
Proportion Criteria (must add 1)	Cost	Volume	Weight	Cost	Volume	Weight	Cost	Volume	Weight	Cost	Volume	Weight
	0.25	0	0.75	0.2	0	0.8	0.2	0	0.8	0.45	0.55	0

	BMW i3 Rex Series PHEV M_1			Toyota Prius Series-Paral.HEV M_1			Hyundai Sonata Paral. HEV M_1		
	Real	Calc	ε[%]	Real	Calc	ε[%]	Real	Calc	ε[%]
Drive Cycle		NEDC			NEDC			NEDC	
Type of Battery or FC	NMC	NMC		NiMH	NiMH	-	LMO	LMO	-
Volume Battery or FC [dm^3]	211	256	**8**	48	48	**0**	47	48	**2**
Weight Battery or FC [kg]	233	283	**8**	41	36	**13**	35	31	**10**
Price Battery or FC [€]	6600	7658	**3**	458	407	**11**	-	504	-
Type of eMotor	hybrid	hybrid		IPM	IPM	-	IPM	IPM	-
Volume eMotor [dm^3]	20	22	**12**	13	13	**4**	10	10	**0**
Weight eMotor [kg]	42	48	**14**	38	43	**15**	35	30	**14**
Price eMotor [€]	-	243	-	-	1432	-	-	1585	-
World g CO_2 [g CO_2/km range]		5915			312			399	
Continent g CO_2 [g CO_2/km range]		5486			291			379	
Proportion Criteria (must add 1)	Cost	Volume	Weight	Cost	Volume	Weight	Cost	Volume	Weight
	0.45	0.55	0	0.25	0	0.75	0.25	0	0.75

	Toyota Mirai FCV M_1				
	Real	Calc	ε[%]	Calc	ε[%]
Drive Cycle		NEDC		EPA	
Type of Battery or FC	FC	FC	-	FC	-
Volume Battery or FC [dm^3]	37	34	**8**	37	**0**
Weight Battery or FC [kg]	56	50	**11**	54	**4**
Price Battery or FC [€]	13552	12322	**9**	13146	**3**
Type of eMotor					
Volume eMotor [dm^3]					
Weight eMotor [kg]					
Price eMotor [€]					
World g CO_2 [g CO_2/km range]		39492		42132	
Continent g CO_2 [g CO_2/km range]		35970		44429	
Proportion Criteria (must add 1)	Cost		Volume		Weight
	0.25		0		0.75

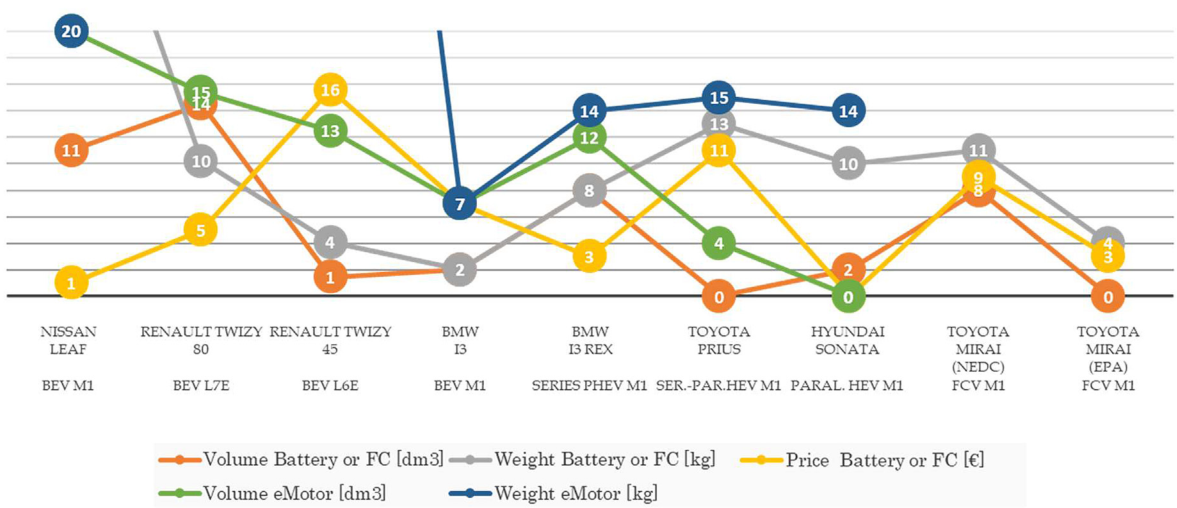

Fig. 21. Dispersion graph of the error values of Table 18.

In addition, the validation has been carried out with several real vehicles that are already on the market, which means that the verification of the method is on a real scale and robust. This is in contrast to validation with a laboratory prototype, which would be more subject to external conditions. Despite this, the methodology works and the results are very promising. The application will also be considered useful for future vehicles of any of the described configurations (EV, series, parallel, and series-parallel (P)HEV, and FCV) and categories (L6e, L7e, M_1, N_1, and LSV).

Taking into account the results obtained, this procedure can be easily transferred to a commercial product thanks to a characterized technology database with its specifications because a prediction of the best option for a vehicle design can be reached based on its design preferences or requirements of ESS and electric motor.

This procedure transforms its input data into easily usable information through the creation of a parts data feedback platform and interactions of OEMs or similar entities with this system can be assessed to evaluate its viability and value in supporting manufacturer decision making.

Future work

Future research work is going to focus on extending the casuistry in relation to vehicle configurations and the number of components that make up the drive train of an EV, (P)HEV and FCV. It is also planned to develop an application with the developed procedure and software.

Formatting of funding sources

This research did not receive any specific grant from funding agencies in the public, private, commercial, or not-for-profit sectors.

Authors contributions

Désirée Alcázar-García: Investigation, Conceptualization, Methodology, Software, Validation, Writing. **José Luis Romeral Martínez**: Supervision.

Declaration of competing interest

The authors declare that they have no known competing financial interests or personal relationships that could have appeared to influence the work reported in this paper.

References

[1] Murray P, Carmeliet J, Orehounig K. Multi-objective optimisation of power-to-mobility in decentralised multi-energy systems. Energy 2020;205:117792. https://doi.org/10.1016/j.energy.2020.117792.
[2] Ahn JH, Kim TS. Effect of oxygen supply method on the performance of a micro gas turbine-based triple combined cycle with oxy-combustion carbon capture. Energy 2020;211:119010. https://doi.org/10.1016/j.energy.2020.119010.
[3] Albrecht FG, Nguyen T-V. Prospects of electrofuels to defossilize transportation in Denmark – a techno-economic and ecological analysis. Energy 2020;192:116511. https://doi.org/10.1016/j.energy.2019.116511.
[4] Xu J-H, Guo J-F, Peng B, Nie H, Kemp R. Energy growth sources and future energy-saving potentials in passenger transportation sector in China. Energy 2020;206:118142. https://doi.org/10.1016/j.energy.2020.118142.
[5] Shanu PN, Senthilkumar S. Performance optimization of mild hybrid passenger vehicle by dual control strategy for city driving cycle. Energy 2021;214:118953. https://doi.org/10.1016/j.energy.2020.118953.
[6] Ju F, Zhuang W, Wang L, Zhang Z. Comparison of four-wheel-drive hybrid powertrain configurations. Energy 2020;209:118286. https://doi.org/10.1016/j.energy.2020.118286.
[7] Global EV Outlook. 2019. Scaling-up the transition to electric mobility. Paris: International Energy Agency (IEA); 2019. https://www.iea.org/reports/global-ev-outlook-2019.
[8] Keller V, Lyseng B, Wade C, Scholtysik S, Fowler M, Donald J, Palmer-Wilson K, Robertson B, Wild P, Rowe A. Electricity system and emission impact of direct and indirect electrification of heavy-duty transportation. Energy 2019;172:740–51. https://doi.org/10.1016/j.energy.2019.01.160.
[9] Correa G, Muñoz P, Rodríguez C. A comparative energy and environmental analysis of a diesel, hybrid, hydrogen and electric urban bus. Energy 2019;187:115906. https://doi.org/10.1016/j.energy.2019.115906.
[10] Ren X, Zhang H, Hu R, Qiu Y. Location of electric vehicle charging stations: a perspective using the grey decision-making model. Energy 2019;173:548–53. https://doi.org/10.1016/j.energy.2019.02.015.
[11] Wappelhorst S. The end of the road? An overview of combustion engine car phase-out announcements across Europe. International Council On Clean Transportation; 2020. https://theicct.org/sites/default/files/publications/Combustion-engine-phase-out-briefing-may11.2020.pdf.
[12] Vichard L, Ravey A, Venet P, Harel F, Pelissier S, Hissel D. A method to estimate battery SOH indicators based on vehicle operating data only. Energy 2021;225:120235. https://doi.org/10.1016/j.energy.2021.120235.
[13] Shaobo X, Qiankun Z, Xiaosong H, Yonggang L, Xianke L. Battery sizing for plug-in hybrid electric buses considering variable route lengths. Energy 2021;226:120368. https://doi.org/10.1016/j.energy.2021.120368.
[14] Li K, Chou F-C, Yen J-Y. Real-time energy-efficient traction allocation strategy for the compound electric propulsion system. IEEE ASME Trans Mechatron 2017;22(3):1371–80. https://doi.org/10.1109/TMECH.2017.2667725.
[15] Arruda BA, Santos MM, Keshri RK. A comparative study of performance for electric vehicles for wheel traction configurations. In: IEEE 25th international symposium on industrial electronics (ISIE); 2016. p. 786–92. https://doi.org/10.1109/ISIE.2016.7744990.
[16] Nguyễn B-H, Vo-Duy T, Henggeler Antunes C, Trovão JPF. Multi-objective benchmark for energy management of dual-source electric vehicles: an optimal control approach. Energy 2021;223:119857. https://doi.org/10.1016/j.energy.2021.119857.
[17] Li X, Williamson SS. Efficiency and suitability analyses of varied drive train architectures for plug-in hybrid electric vehicle (PHEV) applications. In: IEEE vehicle power and propulsion conference. Harbin, China: VPPC); 2008. p. 1–6. https://doi.org/10.1109/VPPC.2008.4677773.
[18] Kim I, Kim H. Configuration analysis of plug-in hybrid systems using global optimization. World Electr Vehicle J 2013;6(2):391–404. https://doi.org/10.3390/wevj6020391.
[19] Freyermuth V, Fallas E, Rousseau A. Comparison of powertrain configuration for plug-in HEVs from a fuel economy perspective. SAE Int J Engine 2008;1(1):392–8. https://doi.org/10.4271/2008-01-0461.
[20] Macias A, Kandidayeni M, Boulon L, Trovão J. Fuel cell-supercapacitor topologies benchmark for a three-wheel electric vehicle powertrain. Energy 2021;224:120234. https://doi.org/10.1016/j.energy.2021.120234.
[21] Chen S-Y, Wu C-H, Hung Y-H, Chung C-T. Optimal energy management of a hybrid electric powertrain system using improved particle swarm optimization. Energy 2018;160:154–70. https://doi.org/10.1016/j.energy.2018.06.023.
[22] García A, Monsalve-Serrano J, Martínez-Boggio S, Wittek K. Potential of hybrid powertrains in a variable compression ratio downsized turbocharged VVA Spark Ignition engine. Energy 2020;195:117039. https://doi.org/10.1016/j.energy.2020.117039.
[23] Geng W, Lou D, Wang C, Zhang T. A cascaded energy management optimization method of multimode power-split hybrid electric vehicles. Energy 2020;199:117224. https://doi.org/10.1016/j.energy.2020.117224.
[24] Fu Z-m, Wang B, Zhou P-g. An improved logic threshold approach of energy management for a power-split hybrid electric vehicle. In: Proceedings of the 2013 international conference on advanced mechatronic systems. Luoyang; 2013. p. 244–8. https://doi.org/10.1109/ICAMechS.2013.6681787.
[25] Purnot T. Comparison of electric series-parallel transmission. Eindhoven: TU/e department mechanical engineering; 2007. www.mate.tue.nl.
[26] Thomas J. Drive cycle powertrain efficiencies and trends derived from EPA vehicle dynamometer results. SAE Int J Passeng Cars Mech Syst 2014;7(4):1374–84. https://doi.org/10.4271/2014-01-2562.
[27] Zulkifli SA, Mohd S, Saad N, Aziz ARA. Influence of motor power and efficiency on fuel consumption of retrofit-conversion split-parallel hybrid electric vehicle. In: IEEE vehicle power and propulsion conference. Beijing: VPPC); 2013. p. 1–5. https://doi.org/10.1109/VPPC.2013.6671715.
[28] Commission delegated regulation No. 134/2014 of 16 december. 2013.
[29] Castelli-Dezza F, Galmarini G, Gobbi M, Mauri M. Design and realization of a quadricycle for urban mobility, ninth international conference and exhibition on ecological vehicles and renewable energies (EVER), monte-carlo. https://doi.org/10.1109/EVER.2014.6844112; 2014. 1-8.
[30] Herrera D, Tosetti S, Carelli R. Dynamic modeling and identification of an agriculture autonomous vehicle. IEEE Latin Am Transact 2016;14(6):2631–7. https://doi.org/10.1109/TLA.2016.7555230.
[31] Hyodo J, Aoshima I, Nakamura A, Saito N, Matsuo R. Development of electric drive system for small vehicles. In: World electric vehicle symposium and exhibition (EVS27); 2013. p. 1–5. https://doi.org/10.1109/EVS.2013.6914825.
[32] Grossard M, Kachroudi S, Abroug N. An optimal energy-based approach for driving guidance of full electric vehicles. Hangzhou: IEEE International Symposium on Industrial Electronics; 2012. p. 1708–13. https://doi.org/10.1109/ISIE.2012.6237348.
[33] Mignot R, Dubas F, Espanet C, Chamagne D. Design of axial flux PM motor for electric vehicle via a magnetic equivalent circuit. Hammamet: First International Conference on Renewable Energies and Vehicular Technology; 2012. p. 212–7. https://doi.org/10.1109/REVET.2012.6195273.
[34] Tran D-D, Vafaeipour M, El Baghdadi M, Barrero R, Van Mierlo J, Hegazy O. Thorough state-of-the-art analysis of electric and hybrid vehicle powertrains: topologies and integrated energy management strategies. Renew Sustain Energy Rev 2020;119:109596. https://doi.org/10.1016/j.rser.2019.109596.
[35] Hu J, Li J, Hu Z, Xu L, Ouyang M. Power distribution strategy of a dual-engine system for heavy-duty hybrid electric vehicles using dynamic programming. Energy 2021;215:118851. https://doi.org/10.1016/j.energy.2020.118851. Part A.
[36] Guo Q, Zhao Z, Shen P, Zhan X, Li J. Adaptive optimal control based on driving style recognition for plug-in hybrid electric vehicle. Energy 2019;186:115824. https://doi.org/10.1016/j.energy.2019.07.154.
[37] Geng W, Lou D, Wang C, Zhang T. A cascaded energy management optimization method of multimode power-split hybrid electric vehicles. Energy 2020;199:117224. https://doi.org/10.1016/j.energy.2020.117224.
[38] Zhang F, Hu X, Langari R, Wang L, Cui Y, Pang H. Adaptive energy management in automated hybrid electric vehicles with flexible torque request. Energy 2021;214:118873. https://doi.org/10.1016/j.energy.2020.118873.
[39] Lin X, Xia Y, Huang W, Li H. Trip distance adaptive power prediction control strategy optimization for a Plug-in Fuel Cell Electric Vehicle. Energy 2021;224:120232. https://doi.org/10.1016/j.energy.2021.120232.
[40] Guo N, Zhang X, Zou Y, Guo L, Du G. Real-time predictive energy management of plug-in hybrid electric vehicles for coordination of fuel economy and battery degradation. Energy 2021;214:119070. https://doi.org/10.1016/

j.energy.2020.119070.
[41] Shen P, Zhao Z, Zhan X, Li J, Guo Q. Optimal energy management strategy for a plug-in hybrid electric commercial vehicle based on velocity prediction. Energy 2018;155:838–52. https://doi.org/10.1016/j.energy.2018.05.064.
[42] Xie S, Hu X, Qi S, Lang K. An artificial neural network-enhanced energy management strategy for plug-in hybrid electric vehicles. Energy 2018;163: 837–48. https://doi.org/10.1016/j.energy.2018.08.139.
[43] Jinquan G, Hongwen H, Jiankun P, Nana Z. A novel MPC-based adaptive energy management strategy in plug-in hybrid electric vehicles. Energy 2019;175: 378–92. https://doi.org/10.1016/j.energy.2019.03.083.
[44] Gao W, Porandla SK. Design optimization of a parallel hybrid electric powertrain, IEEE vehicle power and propulsion conference. 2005. https://doi.org/10.1109/VPPC.2005.1554609.
[45] Cheng Y, Duan F, Cui S. The design principle of electric motors and drive systems for electric vehicles, vol. 1. Nanjing: International Conference on Electrical Machines and Systems; 2005. p. 802–5. https://doi.org/10.1109/ICEMS.2005.202647.
[46] Millo F, Zhao J, Rolando L, Cubito C, Fuso R. Optimizing the design of a plug-in hybrid electric vehicle from the early phase: an advanced sizing methodology. Comput Aided Design Appl 2015;12(1):22–32. https://doi.org/10.1080/16864360.2015.1077072.
[47] Regulation (EU) No 168/2013 of the European Parliament and of the Council of 15 January 2013 on the approval and market surveillance of two- or three-wheel vehicles and quadricycles.
[48] Directive 2007/46/EC of the European Parliament and of the Council of 5 September 2007 establishing a framework for the approval of motor vehicles and their trailers, and of systems, components and separate technical units intended for such vehicles.
[49] Federal motor vehicle safety standard (FMVSS) 500; 49 CFR 571 vol. 3 , October 1, 2010.
[50] Overington S, Rajakaruna S. A combined high-efficiency region controller to improve fuel consumption of power-split HEVs. IEEE Trans Veh Technol 2016;65(6):4597–607. https://doi.org/10.1109/TVT.2016.2543505.
[51] Anseán D, González M, García VM, Viera JC, Antón JC, Blanco C, Blanco C. Evaluation of LiFePO4 batteries for electric vehicle applications. IEEE Trans Ind Appl 2015;51(2):1855–63. https://doi.org/10.1109/TIA.2014.2344446.
[52] Haubert T. Optimal control of mathematical model of the electrovehicle. Faculty of Electrical Engineering. Department of Electric Drives and Traction. Czech Technical University in Prague; 2015. http://hdl.handle.net/10467/62095.
[53] Alcázar-García D, Romeral Martínez L. Energy consumption and total vehicle efficiency calculation procedure for electric vehicles (EV, HEV and PHEV). In: ASME international design engineering technical conferences and computers and information in engineering conference, 20th international conference on advanced vehicle technologies, quebec city, quebec. Canada; 2018. https://doi.org/10.1115/DETC2018-85182.
[54] Alcázar-García D, Romeral Martínez L. Calculation energy consumption, range and efficiency for different electric, hybrid and fuel cell vehicles. EVS 31 & EVTeC; 2018. https://confit.atlas.jp/guide/event/evs31/subject/F7-03/date?cryptoId=.
[55] Li X, Lopes LAC, Williamson SS. Comparative investigation of series and parallel hybrid electric vehicle efficiencies based on comprehensive parametric analysis. Calgary, AB: IEEE Power & Energy Society General Meeting; 2009. p. 1–8. https://doi.org/10.1109/PES.2009.5275171.
[56] Du J, Chen J, Song Z, Gao M, Ouyang M. Design method of a power management strategy for variable battery capacities range-extended electric vehicles to improve energy efficiency and cost-effectiveness. Energy 2017;121:32–42. https://doi.org/10.1016/j.energy.2016.12.120.
[57] Wieczorek M, Lewandowski M. A mathematical representation of an energy management strategy for hybrid energy storage system in electric vehicle and real time optimization using a genetic algorithm. Appl Energy 2017;192: 222–33. https://doi.org/10.1016/j.apenergy.2017.02.022.
[58] Thomas J. Drive cycle powertrain efficiencies and trends derived from EPA vehicle dynamometer results. SAE Int J Passeng Car Mech Syst 2014;7(4): 1374–84. https://doi.org/10.4271/2014-01-2562.
[59] Weisser D. A guide to life-cycle greenhouse gas (GHG) emissions from electric supply technologies. Energy 2007;32(9):1543–59. https://doi.org/10.1016/j.energy.2007.01.008.
[60] Energy Statistics Pocketbook and country datasheets. United nations. Department of Economic and Social Affairs; 2019. https://unstats.un.org/unsd/energystats/pubs/pocketbook/.
[61] Ramos C, Salomé García A, Moreno B, Díaz G. 2019-Small-scale renewable power technologies are an alternative to reach a sustainable economic growth: evidence from Spain. Energy 2019;167:13–25. https://doi.org/10.1016/j.energy.2018.10.118.
[62] Sakawa M, Kato K, Ushiro S, Inaoka M. Operation planning of district heating and cooling plants using genetic algorithms for mixed integer programming. Appl Soft Comput 2001;1(Issue 2):139–50. https://doi.org/10.1016/S1568-4946(01)00014-X.
[63] Mateos Andaluz A. Algoritmos Evolutivos y Algoritmos Genéticos, Inteligencia en Redes de Comunicaciones. Ingeniería de Telecomunicación. Universidad de Carlos III; 2009. https://docplayer.es/44761469-Algoritmos-evolutivos-y-algoritmos-geneticos.html.
[64] Winter Althaus G. Las matemáticas del siglo XX una mirada en 101 artículos - algoritmos genéticosmétodos estocásticos de optimización global inspirados en la evolución natural: incidencias en el progreso tecnológico. Universidad de La Laguna: Sociedad Canaria Isaac Newton de Profesores de Matemáticas: Nivola; 2000. p. 385. https://dialnet.unirioja.es/servlet/libro?codigo=937.
[65] Alba E, Laguna M, Martí R. Métodos evolutivos. Ingeniería UC (Venezuela) 2003;10(3):80–9. https://www.researchgate.net/publication/228359112_Metodos_Evolutivos.
[66] Cui H, Xiao G. Fuel-efficiency technology trend assessment for LDVs in China: hybrids and electrification. The International Council on Clean Transportation; 2018. https://theicct.org/publications/fuel-efficiency-tech-china-electrification.
[67] James BD, Huya-Kouadio JM, Houchins C, DeSantis DA. Mass production cost estimation of direct H2 PEM fuel cell systems for transportation applications: 2018 update. Strategic Analysis Inc.; 2018. https://www.energy.gov/sites/prod/files/2020/02/f71/fcto-sa-2018-transportation-fuel-cell-cost-analysis-2.pdf.
[68] Schmidt O, Hawkes A, Gambhir A, Staffell I. The future cost of electrical energy storage based on experience rates. Nat Energy 2017;2:17110. https://doi.org/10.1038/nenergy.2017.110.
[69] Stephan F. Baterías de Litio Solar. Estatus del mercado en Alemania, Deutsche Gesellschaft für Internationale Zusammenarbeit (GIZ) GmbH. 2018. www.burof.de.
[70] Wang J. Battery electric vehicle energy consumption modelling, testing and prediction: a practical case study. Eindhoven: Eindhoven University of Technology; 2016. https://pure.tue.nl/ws/files/41303833/20161031_Wang.pdf.
[71] Thielmann DA, Sauer A, Isenmann PDR, Wietschel PDM. Technology roadmap energy storage for electric mobility 2030. Fraunhofer Institute for Systems and Innovation Research ISI. Competence Center Emerging Technologies; 2013. https://www.isi.fraunhofer.de/content/dam/isi/dokumente/cct/lib/TRM-ESEM-2030_en.pdf.
[72] Electrical and Electronics Technical Team Roadmap. US drive, driving research and innovation for vehicle efficiency and energy sustainability. 2017. https://www.energy.gov/eere/vehicles/downloads/us-drive-electrical-and-electronics-technical-team-roadmap.
[73] Hutchinson T, Burgess S, Herrmann G. Current hybrid-electric powertrain architectures: applying empirical design data to life cycle assessment and whole-life cost analysis. Appl Energy 2014;119:314–29. https://doi.org/10.1016/j.apenergy.2014.01.009.
[74] Widmer JD, Martin R, Kimiabeigi M. Electric vehicle traction motors without rare earth magnets. Sustain Mater Technol 2015;3:7–13. https://doi.org/10.1016/j.susmat.2015.02.001.
[75] Duleep G, van Essen H, Kampman B, Grünig M. Assessment of electric vehicle and battery technology. Impacts of Electric Vehicles - deliverable 2. Delft: ICF/CE Delft/Ecologic Institute; 2011. https://www.ecologic.eu/13512.
[76] Du ZS, Lipo TA. Torque performance comparison between a ferrite magnet vernier motor and an industrial interior permanent magnet machine. IEEE Trans Ind Appl 2017;53(3):2088–97. https://doi.org/10.1109/TIA.2017.2673812.
[77] Ionel DDM. New frontiers of brushless PM motor technology. CWIEME Berlin; 2016. https://www.engineeringspecifier.com/drives-motors/seminar-to-unveil-new-frontiers-of-brushless-pm-motor-technology.
[78] Tekgun B, Husain T, Das S, Sozer Y, Hamd M. Design of a novel interior permanent magnet axial flux machine. Cincinnati, OH: IEEE Energy Conversion Congress and Exposition (ECCE); 2017. p. 314–20. https://doi.org/10.1109/ECCE.2017.8095798.
[79] Miller JM, Electric Motor R&D, U.S. DOE. Hydrogen and fuel. Cells program and vehicle technologies program annual merit review and peer evaluation meeting. Oak Ridge National Laboratory; 2013. https://www.energy.gov/sites/prod/files/2014/03/f13/ape051_miller_2013_o.pdf.
[80] Burress T. Benchmarking of competitive technologies, U.S. DOE hydrogen and fuel cells program and vehicle technologies. Oak Ridge National Laboratory; 2011. https://www.energy.gov/sites/prod/files/2014/03/f10/ape006_burress_

2011_o.pdf.
[81] Samsun R, Antoni L, Rex M. Mobile fuel cell application: tracking market trends. IEA Advanced Fuel Cells Technology Collaboration Programme; 2020. https://www.ieafuelcell.com/fileadmin/publications/2020_AFCTCP_Mobile_FC_Application_Tracking_Market_Trends_2020.pdf.
[82] Yoshida T, Kojima K. Toyota MIRAI fuel cell vehicle and progress toward a future hydrogen society. Electrochem Soc Interf 2015;24. https://doi.org/10.1149/2.F03152if. Number 2.
[83] Gray T, Wishart PJ, Shirk M. 2011 nissan Leaf VIN 0356 electric vehicle battery test results. U.S. Department of Energy. Energy Efficiency and Renewable Energy.; 2016. https://avt.inl.gov/sites/default/files/pdf/fsev/batteryrpt2011NissanLeaf0356.pdf.
[84] Schöwel D-IF, Hockgeiger D-IE. The High Voltage Batteries of the BMW i3 abd BMW i8. ATLANTA: AABC; 2014. https://wiki.aalto.fi/download/attachments/91692283/high_voltage_batteries_of_bmw_vehicles.pdf?version=1&modificationDate=1398446470505&api=v2.
[85] Gray T, Shirk M, Wishart J. Hyundai Sonata hybrid − advanced vehicle testing − baseline testing results. U.S. Department of Energy. Energy Efficiency and Renewable Energy; 2011−13. https://www.energy.gov/sites/prod/files/2014/02/f7/batterysonata4932_2.pdf.
[86] Hofman T, van Druten R, Serrarens A, van Baalen J. A fundamental case study on the Prius and IMA drivetrain concepts. The Netherlands: Technische Universiteit Eindhoven and Drivetrain Innovations BV; 2005. https://www.researchgate.net/publication/228965631_A_fundamental_case_study_on_the_Prius_and_IMA_drivetrain_concepts.
[87] Lequesne B. Electric machines for automotive propulsion: history and future, ITEC Asia-Pacific. 2019. www.emotorseng.com.
[88] Li J. Adaptive model-based state monitoring and prognostics for lithium-ion batteries. Germany: Universität Ulm, Baden Würtemberg; 2016. https://oparu.uni-ulm.de/xmlui/handle/123456789/4157.
[89] Electric motors technical data of letrika. 2021. http://www.letrika.com/katalog.